

Nanowire Piezo-phototronic Photodetector: Theory and Experimental Design

Ying Liu, Qing Yang, Yan Zhang, Zongyin Yang, and Zhong Lin Wang*

The piezo-phototronic effect is a new field of research that utilizes the three-way coupling of piezoelectricity, photoexcitation and semiconductor properties of the same material to enhance its performance for optoelectronic devices.^[1,2] Its core physics relies on the modification effect of the piezoelectric potential (piezopotential) on the band structure at a contact or junction for effective tuning/controlling of the charge transport. Materials that exhibit the piezo-phototronic effect are mainly in the Wurtzite family, such as ZnO, CdS, GaN, InP, etc.^[3–6] The one-dimensional structures of these materials are ideal for fabricating strain-controlled piezo-phototronic devices. The strain applied to cause the deformation of the nanowires is mainly through shape change of the flexible substrate that supports the device. Such devices can be the basis for active flexible electronics, which uses the mechanical actuation from the substrate for inducing new electronic/optoelectronic effects.

As the piezopotential is controlled by externally applied mechanical deformation with different orientation and magnitude, the piezo-phototronics effect can be combined with flexible optoelectronics to promote new device functions. Previously, we have demonstrated the enhancement of the sensitivity of UV photodetector,^[6] the response of photocells,^[7] and the emission efficiency of light emitting diodes.^[8] In these reports, the coupling between piezoelectric effect and photoexcitation has been investigated experimentally. Theoretical calculation of the piezopotential along ZnO nanowires under different strain has been carried out,^[9–11] and a theoretical framework has been built for the two-way coupling between the piezoelectric effect and semiconductor transport properties.^[12]

Theoretical study for the three-way coupling in piezo-phototronics remains to be investigated. Constructing such a model will not only provide an in-depth understanding about the experimental results, but also explore the core phenomena and build high performance devices. Besides piezo-phototronic effect, other factors such as piezoresistance effect and change of contact area or contact condition can also affect the device performance. It is important to distinguish the contribution

made by the piezo-phototronics effect from these other factors through theoretical analysis.

In this paper, we have constructed a theoretical model and fabricated corresponding experimental devices to study the piezo-phototronic photodetectors based on single-Schottky and double-Schottky contacted metal–semiconductor–metal (MSM) structures. We have coupled the photoexcitation and piezoelectric terms into basic current equations to study their influence on the final device performance. Theoretically predicted results have been quantitatively verified by photodetectors based on CdS nanowires for visible light and ZnO nanowires for UV light. Our experimental results show that the piezo-phototronic effect dominates the performance of the photodetector rather than other experimental factors. It is shown that the piezo-phototronic effect is significantly pronounced at low light intensities, which is important for extending the sensitivity and application range of the photodetector. The conclusions drawn on Schottky contacts present the core properties of the effect and can easily be extrapolated to other structures like p-n junctions. Finally, based on the theoretical model and experimental results, we have proposed three criteria for describing the contribution made by the piezo-phototronic effect to the performance of the photodetectors, which are useful for distinguishing this effect from other factors in governing the performance of the photodetector.

The theoretical model for two-way coupling in piezotronics has been developed in a previous report.^[12] Here we adopt the same assumptions and follow similar methods, as schematically shown in **Figure 1**. The depletion approximation is assumed for the Schottky contact. Piezoelectric polarization is induced in a semiconductor nanowire when it is subjected to strain, it is reasonable to assume that the piezo charges are distributed in a layer in the depletion zone, which tune the Schottky barrier height. The formation of an inner potential will drive the free charge carriers to redistribute. If there is no external bias, the inner electric field and net charges should only exist in the depletion zone at static or quasi-static state. The Schottky contact current equation will be used as the basic starting point. The influence of photoexcitation and piezo-charges on the material band structure will be discussed, and the final coupled term will be integrated into the current transport equation. To give more intuitive perspective of the piezo-phototronic effect, we have also carried out numerical simulations. A one-dimensional model and other simplifications are adopted for easy understanding. The core equations and conclusions are shown in the analytical model below.

Current Density for a Forward Schottky Contact: For a piezo-phototronic photodetector, a measurement of the photon-induced current is an indication of photon intensity. The coupling effect of piezoelectricity and photon excitation is also

Y. Liu,^[+] Dr. Q. Yang,^[+] Dr. Y. Zhang, Prof. Z. L. Wang
School of Material Science and Engineering
Georgia Institute of Technology
Atlanta, Georgia, 30332-0245, United States
E-mail: zlwang@gatech.edu

Dr. Q. Yang, Dr. Z. Y. Yang
State Key Laboratory of Modern Optical Instrumentation
Department of Optical Engineering
Zhejiang University
Hangzhou 310027, P. R. China

[+] Y.L. and Q.Y. contributed equally in this work.



DOI: 10.1002/adma.201104333

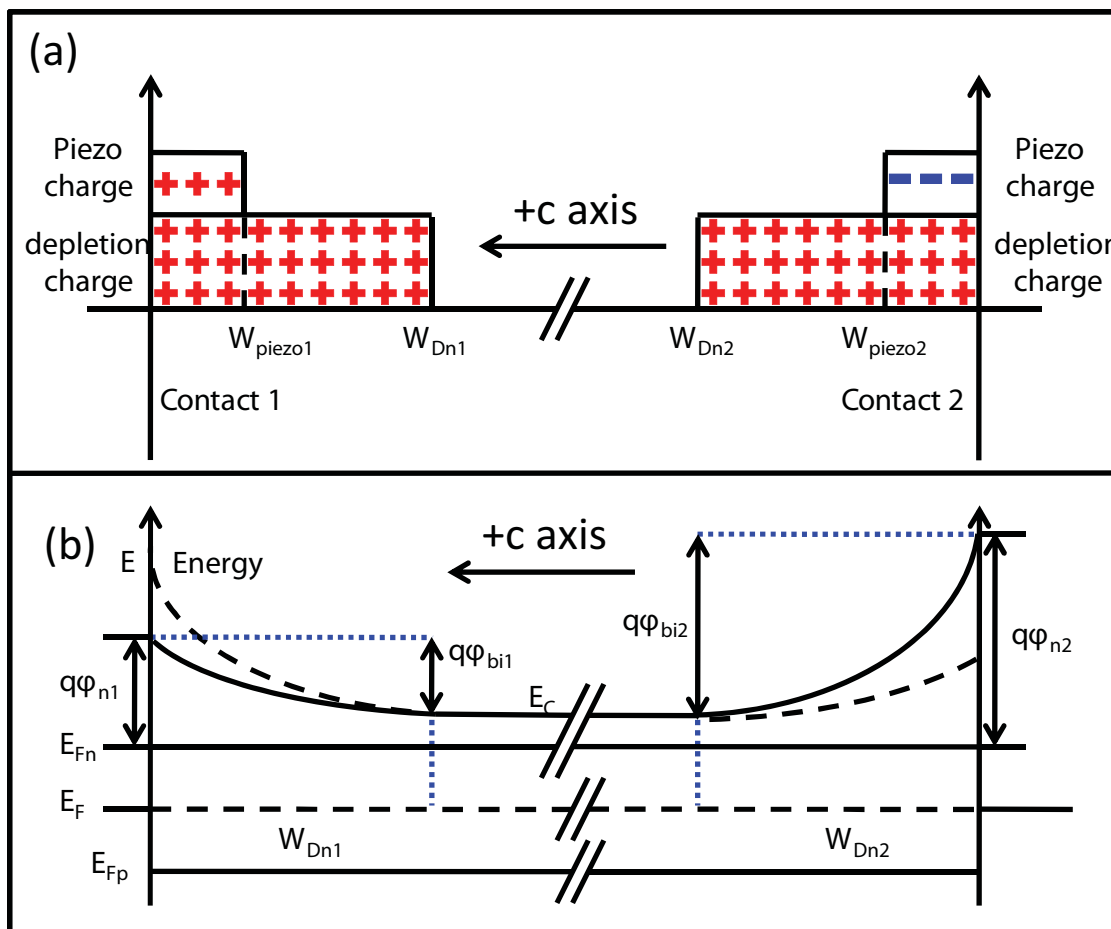


Figure 1. Illustration of ideal metal–semiconductor–metal structures with the presence of piezo-charges and photon generated charges. (a) Space charge distribution and corresponding (b) energy band diagram in the presence of piezo charges and photo generated charges. Dashed lines stand for original barriers without strain nor photoexcitation. The solid line is the finally tuned band structure by the piezo-charges, with one end being lifted up and one side being lowered.

studied as a strain being applied. For an n-type Schottky contacted device between a metal and a semiconductor under forward bias voltage, the thermionic emission (TE) theory should be adopted for the charge carrier transport, and the current density under forward bias J_F is^[13]

$$J_F = A^* T^2 e^{-\frac{q}{kT} \phi_n} \left(e^{\frac{qV}{kT}} - 1 \right) \quad (1)$$

where A^* is the Richardson constant, T is temperature, q is electron charge, ϕ_n is the effective Schottky barrier height, and V is the applied voltage across the contact.

Current Density for a Reversely Biased Schottky Contact: For a reversely biased n-type Schottky contact, the TE theory underestimates the current, but the thermionic field emission (TFE) theory which takes into account the tunneling effect describes the behavior of heavily doped semiconductor materials better.^[13,14] According to the TFE theory, the current density under reverse bias takes the form of

$$J_R = J_{sv} e^{-\frac{q}{E_0} \phi_n} e^{V_R \left(\frac{q}{kT} - \frac{q}{E_0} \right)} \quad (2)$$

where J_{sv} is the slowly varying term regarding applied voltage and Schottky barrier change, V_R is the reverse voltage, q is electron charge, k the Boltzmann constant, and E_0 is a tunneling parameter of the same order of but larger than kT .^[15] Usually E_0 is larger than kT , and is constant regarding barrier height and applied voltage, so it is reasonable to assume that $E_0 = akT$, with $a > 1$, so equation (2) now becomes

$$J_R = J_{sv} e^{-\frac{q}{akT} \phi_n} e^{V_R \frac{q}{kT} \left(1 - \frac{1}{a} \right)} \quad (3)$$

Equations for Photoexcitation: Photons with energy higher than the bandgap (E_g) of the photodetector material will excite electron-hole pairs. Under a steady light illumination, the excess free carrier concentration is constant. The excess carrier concentration is given by the continuity equation^[16]

$$\Delta n = \Delta p = \tau_n G_L(I) \quad (4)$$

where Δn is the excess electron concentration and Δp the excess hole concentration under light illumination, τ_n is the carrier lifetime, and $G_L(I)$ is the rate of photon generation, which is a function of light intensity.

Without photoexcitation the Fermi level of the semiconductor lines up with the Fermi level of the metal. When a nanowire is illuminated, the existence of excess carriers will result in a split of the original Fermi level into two quasi-Fermi levels for electrons and holes accordingly, as shown in Figure 1b. As long as the light illumination is uniform, the quasi Fermi level should also be uniform along the entire nanowire. The quasi Fermi level E_{F_n} for electrons and E_{F_p} for holes can be described by^[13]

$$E_{F_n} = E_F + kT \ln \left(\frac{n_0 + \Delta n}{n_0} \right) \quad (5-1)$$

$$E_{F_p} = E_F - kT \ln \left(\frac{p_0 + \Delta p}{p_0} \right) \quad (5-2)$$

Equations for Piezo-charges and Piezopotential: As in previous theoretical frame work for piezotronics,^[12] the modification to the Schottky barrier height by piezo-charges is

$$\Delta\varphi_{piezo} = -\frac{1}{2\epsilon} \rho_{piezo} W_{piezo}^2 \quad (6)$$

where ρ_{piezo} is the density of the strain-induced piezo-charges at the nanowire side of the metal–semiconductor junction, and W_{piezo} is the width of the piezo-polar charge distribution adjacent to the interface.

As piezoelectricity originated from inner crystal polarization of ions, the piezo-charges can be seen as fixed charges at the two ends of the nanowire with opposite signs, which is shown in Figure 1a. For a Wurtzite structured nanowire with strain along the c -axis, which is assumed to be the growth direction of the nanowire, the piezo polarization is

$$P = e_{33}S_{33} = \rho_{piezo1} W_{piezo1} = -\rho_{piezo2} W_{piezo2} \quad (7)$$

where e_{33} stands for the piezoelectric constant, and S_{33} stands for the strain along the c -axis, ρ_{piezo1} is the density of the strain-induced piezo-charges at contact 1, and ρ_{piezo2} is the density of the strain-induced piezo-charges at contact 2.

Piezo-Phototronics Effect for a Single Schottky Contact: For a Schottky contact, photo excitation can effectively reduce the height of the Schottky barrier, while the introduction of local piezo-charges can change the barrier height, which can be quantitatively expressed as

$$\Delta\varphi_n = -\frac{1}{2\epsilon} \rho_{piezo} W_{piezo}^2 - \frac{kT}{q} \ln \left(\frac{n_0 + \Delta n}{n_0} \right) \quad (8)$$

Thus, the modified barrier height is

$$\varphi_n = \varphi_{n0} + \Delta\varphi_n \quad (9)$$

where φ_{n0} is the original Schottky barrier height without strain nor light illumination.

The electron current density transported through a forwardly biased Schottky contact is then

$$J_n = J_{n0} \left(\frac{n_0 + \Delta n}{n_0} \right) \exp \left(\frac{q}{kT} \frac{1}{2\epsilon} \rho_{piezo} W_{piezo}^2 \right) \quad (10)$$

where J_{n0} is the current density without applying light illumination nor external strain, and $J_{n0} = A^* T^2 e^{-\frac{q}{kT} \varphi_{n0}} (e^{\frac{q}{kT} V} - 1)$

As the sign of ρ_{piezo} depending on the direction of c -axis and type of applied strain, the presence of the piezo-charges can either enhance device current or reduce it depending to the orientation of the nanowire.

Piezo-Phototronics Effect for a Double-Schottky-Contact Structure: In a device with double Schottky contacts, under certain bias voltage, one junction will be reversely biased and the other junction will be forwardly biased. The current across the double Schottky junction device should take the form:

$$I = S_R J_R = V_{NW} / R_{NW} = S_F J_F \quad (11)$$

where S_R and S_F are cross section area for reverse junction and forward junction accordingly, R_{NW} is the resistance of the nanowire, and V_{NW} is the voltage across the nanowire. Thus, we have:

$$V_R + V_{NW} + V_F = V \quad (12)$$

where V_R and V_F are the voltage across the reverse and forward junction, V is the total applied voltage.

In Equation (11), the R_{NW} term mainly influences the current behavior at applied voltage above 5 V or higher,^[15] and at working voltage range for photodetection, the dominating term should be mainly controlled by the reversely biased contact. To clearly see the effect of piezo-charges and photo excitation, we make reasonable simplifications that $V_R = cV$, where c is assumed constant and $c < 1$. Thus, Equation (3) now becomes:

$$J = J_{sv} \exp \left(-\frac{q}{akT} \varphi_{n0} \right) \exp \left[V \frac{q}{kT} c \left(1 - \frac{1}{a} \right) \right] \left(\frac{n_0 + \Delta n}{n_0} \right)^{\frac{1}{a}} \exp \left(\frac{q}{akT} \frac{1}{2\epsilon} \rho_{piezo} W_{piezo}^2 \right) \quad (13)$$

Thus, the device current under different bias voltage takes the form

$$I = S_1 J_{C1} \left(\frac{n_0 + \Delta n}{n_0} \right)^{\frac{1}{a}} \exp \left(\frac{q}{akT} \frac{1}{2\epsilon} \rho_{piezo1} W_{piezo1}^2 \right) \quad \text{when contact 1 is under reverse bias } (V > 0) \quad (14-1)$$

$$I = -S_2 J_{C2} \left(\frac{n_0 + \Delta n}{n_0} \right)^{\frac{1}{a}} \exp \left(-\frac{q}{akT} \frac{1}{2\epsilon} \rho_{piezo2} W_{piezo2}^2 \right) \quad \text{when contact 2 is under reverse bias } (V < 0) \quad (14-2)$$

where $J_{C1} = J_{sv1} \exp \left(-\frac{q}{a_1 kT} \varphi_{n10} \right) \exp \left[V \frac{q}{kT} c_1 \left(1 - \frac{1}{a_1} \right) \right]$ and $J_{C2} = J_{sv2} \exp \left(-\frac{q}{a_2 kT} \varphi_{n20} \right) \exp \left[V \frac{q}{kT} c_2 \left(1 - \frac{1}{a_2} \right) \right]$ are the currents under reverse bias for contact 1 and 2 accordingly, and S_1 and S_2 are the areas for junction 1 and 2, respectively. As ρ_{piezo1} and ρ_{piezo2} have opposite signs, Equation (14) shows asymmetric change in photocurrent under opposite bias by the same amount of applied strain.

Numerical Simulation of a MSM Photodetector: We now apply our analytical results to numerical calculation for a Ag-CdS-Ag structure. As the materials for piezo-phototronics are mainly Wurtzite structured materials such as CdS, ZnO and GaN, who share the same crystal symmetry, their piezoelectric coefficient matrix takes the same form.

The parameters for CdS are as follows: dielectric constant $\epsilon = \epsilon_s \epsilon_0$, with $\epsilon_s = 9.3$,^[17] and piezoelectric coefficient $e_{33} = 0.385$ C/m³. The distribution width of piezo charges W_{piezo} is assumed 1 nm. The relationship between illumination power

and photo current is given by the following equation as well as Equation (4):

$$\frac{I_{ph}}{P_{ill}} = \frac{\eta_{ext}q}{h\nu} \Gamma_G \quad (15)$$

where I_{ph} is the photo current, P_{ill} is the illumination power, which is related to excitation power and the diameter of the wire as well as, and the spacing between the two electrodes; η_{ext} is the external quantum efficiency; q is the electron charge; h the Planck constant, ν the light frequency, and Γ_G the internal gain. In the photoexcitation process, Γ_G and η_{ext} relates to the value of $G_L(l)$ in equation (4). For photoexcitation, we assume $\eta_{ext} = 1$, $\Gamma_G = 1.5 \times 10^5$,^[6] carrier lifetime $\tau_n = 3.6$ ns.^[18] For typical visible light photodetection experiments, the light wavelength $\lambda = 486$ nm. At dark condition, the electron concentration in CdS nanowire is assumed to be 1×10^{15} cm⁻³. The size of the nanowire does not affect the calculation in our model, unless the diameter is small enough for quantum effect to occur.

For a Ag-CdS-Ag structure with one Ohmic contact and one Schottky contact, we are able to calculate the photocurrent under the same intensity of light illumination with applied strain varying from 0 to 1% when forward bias is applied on the Schottky contact, using Equation (10). Depending on the direction of c -axis, the photocurrent can either increase or decrease with applied strain. Figure 2a and Figure 2b shows the performance of two single-Schottky-contact devices, the configuration of which are shown in the inset of Figure 2a and Figure 2b accordingly. We are also able to calculate the photocurrent under strain-free conditions with different illumination power, as shown in Figure 2c.

For a Ag-CdS-Ag structure with two Schottky contacts at both ends, we set $a = 1.3$ and $c = 0.8$ in Equation (13), which are reasonable values according to previous reports.^[15] The result of the according simulation is shown in Figure 3. In Figure 3a, the asymmetric characteristic of the piezo-phototronic effect is demonstrated very clearly: the change of current under the same amount of applied strain is opposite when the bias voltage is applied at the opposite direction. Figure 3b shows that under different illumination power, the photocurrent changes symmetrically with regard to the two Schottky contacts.

For ZnO, the dielectric constant $\epsilon_s = 8.9$, piezoelectric coefficient $e_{33} = 1.22$ C/m³, carrier lifetime $\tau_n = 3.0$ ns.^[19] which means that the simulation results for ZnO will only have a slight difference in magnitude with CdS, and will have the same trends of change with strain and light intensity. Numerical simulation for ZnO photodetection is also carried out and shown in Figure 4.

To further verify our model, we have designed experiments to study the CdS nanowire based photodetectors. CdS has a band gap of ~ 2.4 eV, which corresponds to excitation wavelength ~ 520 nm. Thus, CdS can be utilized for detection of visible light. CdS nanowires have Wurtzite crystal structures, which is the same as ZnO nanowires, so their piezoelectric coefficient tensor and other crystal symmetry related parameters take similar forms.

Device Fabrication and Measurement: Our CdS nanowires were synthesized using high-temperature thermal evaporation process, and are typically 1 to 3 micrometers in diameter and several hundreds of micrometers in length.^[20,21] The photodetectors

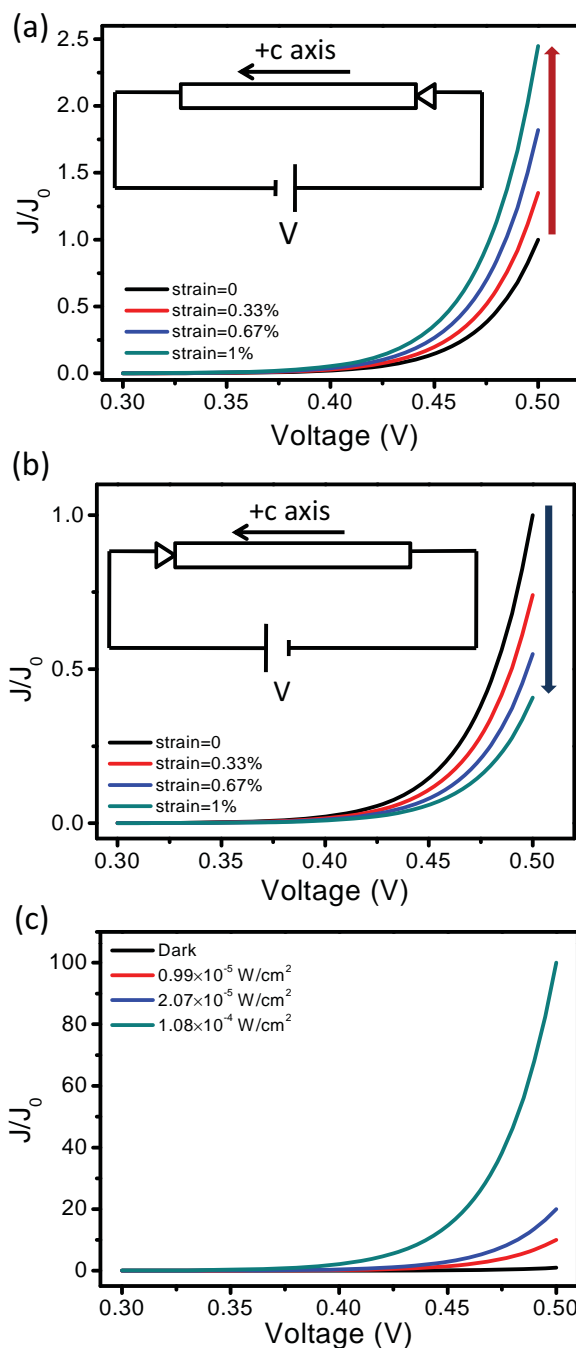


Figure 2. Results for numerical simulation for a metal-CdS-metal photodetector with a Schottky contact on one end and Ohmic contact on the other end based on our analytical solution. (a,b) Relative current density versus voltage under different strains and the same illumination power, for two devices with different orientation of c -axis regarding the position of the Schottky contact. J_0 is set as the current of the device at zero strain and at applied voltage of 0.5 V. Insets are the configuration of device and direction of forward bias. (c) Current-voltage diagram under different illumination power. J_0 is set for the dark current at forward applied voltage of 0.5 V.

are fabricated in a similar way as reported previously:^[6] a single CdS nanowire is placed on an elastic Kapton (polyimide) substrate with a size of around 20 mm \times 8 mm \times 0.5 mm, with

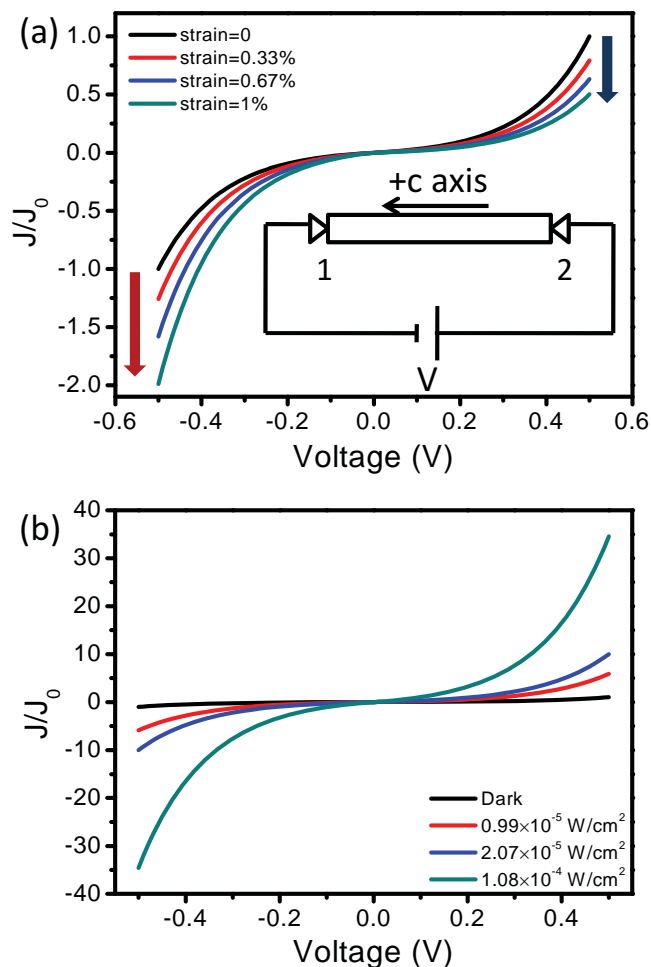


Figure 3. Numerical simulation for a metal-CdS-metal photodetector with Schottky contact on both ends based on our analytical solution. (a) Relative current density vs. voltage under different strains and the same illumination power. J_0 is set as the current of the device at zero strain and at reverse applied voltage of 0.5 V. Inset is the configuration of device and direction of forward bias. (b) current-voltage diagram under different illumination power. J_0 is set for the dark current at forward applied voltage of 0.5 V.

both ends bonded to the substrate and copper wires using silver paste. The device is placed upside-down onto a Nikon Eclipse Ti inverted microscope system, which can monitor and excite the photon detection. A 3D stage with a movement resolution of 1 μm is placed on top of the device to apply mechanical force, and it induces tensile strain in the longitudinal direction of the nanowire. In this microscope system the excitation light source is a Nikon Intensilight C-HGFIE lamp, and a remote controller and neutral density filters is used to adjust illumination power. For the CdS photodetector, blue light with a center wavelength of 486 nm is used. The light beam is focused onto the nanowire using a 10 \times magnifying lens. Current–voltage measurements are carried out using a Keithley 487 picoammeter/voltage source in conjunction with a GPIB controller (National Instruments GPIB-USB-HS, NI 488.2). The schematic diagram of the experiment method is shown in Figure S1.

Experimental Results and Comparison with Calculation: Our experimental results shows two kinds of typical MSM photodetectors, single Schottky contact photodetector and double Schottky contact photodetector. **Figure 5** is the result for a single Schottky contact photodetector. As shown in Figure 5b, the current decreases under increasing strain. Thus, the device configuration and direction of the c -axis is as shown in the inset of Figure 5b. In Figure 5d, the change of responsivity R with applied strain for the photodetector is calculated while the illumination power is kept at $6.4 \times 10^{-6} \text{ W/cm}^2$. Responsivity is the measurement of degree of sensitivity, and we have $R = \frac{I_{ph}}{P_{ill}}$, where I_{ph} is the photo current, P_{ill} is the illumination power, which is the measurement of light intensity. We can see that the responsivity in this case decreases with positive strain. As the piezo-phototronic effect is asymmetric and direction-sensitive, the direction of the c -axis should be taken into consideration in device fabrication with a single Schottky contact in order to get an enhancement rather than a decrease in device performance. In Figure 5c it is shown that the rectifying current–voltage behavior has changed to a nearly symmetric behavior when the illumination power increases to as high as 0.24 W/cm^2 . This can be explained by the increase of the quasi-Fermi level, which leads to a quick breakdown of the Schottky contact under a reversely biasing voltage.

Figure 6 is the result for a double Schottky contact photodetector. As shown in Figure 6b, the change in I – V characteristic with applied strain is in the way exactly as predicted by the theoretical model: while the current under forward bias increases with applied strain, under reverse bias the current decreases with it. Our experiments on ZnO nanowire based photodetector for UV light also fit the theory nicely (Figure 4d).

In both Figure 5c and Figure 6c, we can see that, with an increase in illumination power, the strain effects are not as significant as that at lower illumination power. As the piezo-charges are independent of illumination power, and change in Fermi level at higher illumination power can dictate the change in Schottky barrier height. With higher light density, the I – V characteristic of the photodetector gets closer to a linear behavior, because the photo excited excess charge carrier density Δn can be significantly larger than the intrinsic charge carrier due to doping, and the quasi-Fermi level for electrons gets much higher than the Fermi level of the metal, whereas charge redistribution also takes place, which can reduce the depletion region and lower the effective Schottky barrier height. Thus, the Schottky barrier height gets so low that their behaviors are very close to the linear behavior of Ohmic contact, and the influence of piezo charges are not as significant as lower illumination power conditions. Therefore, the piezo-phototronic effect can help enhance sensitivity of the detection at low light intensity, but does not necessarily have significant effect for strong light intensity. In practice, the detection of low intensity light is practically desired.

However, several other factors needs to be considered as well:

1) Effect of piezoresistance

When a crystal lattice is deformed under strain, the band gap width shall have a minor change, and can finally result in conductance change of the semiconductor. This is called the piezoresistance effect.^[22,23] The piezoresistance effect is present in semiconductors either with or without piezoelectricity. In

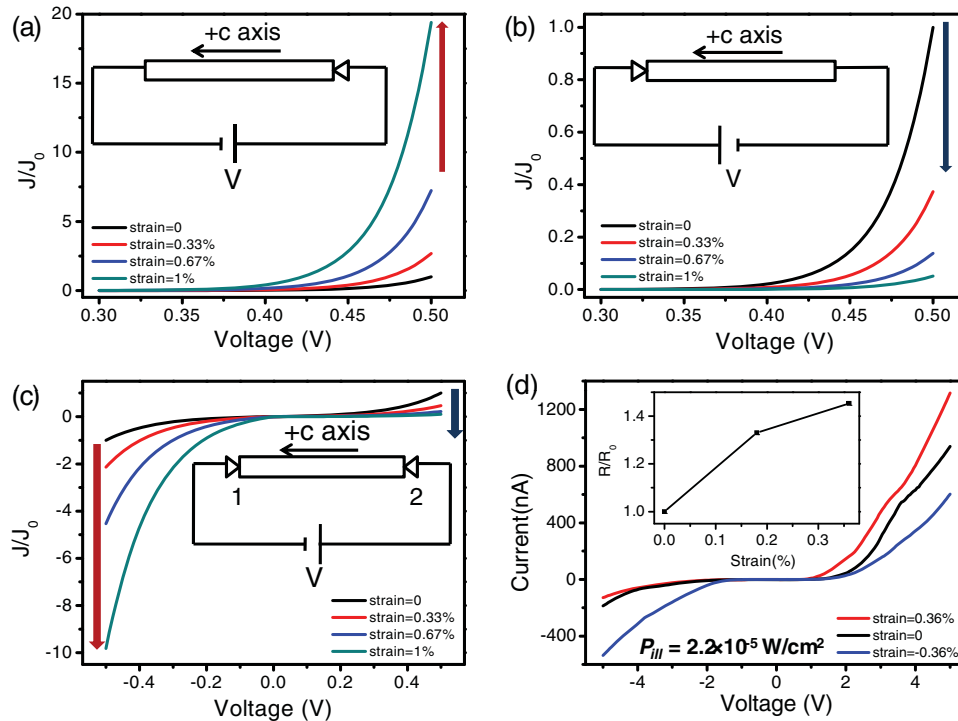


Figure 4. Numerical calculation regarding photodetection of Ag-ZnO-Ag structure. (a) (b) are relative current density vs. voltage under different strains and the same illumination power, for two devices with different orientation of *c*-axis regarding the position of the Schottky contact. J_0 is set as the current of the device at zero strain and at applied voltage of 0.5 V. Insets are the configuration of device and direction of forward bias. (c) Relative current density vs. voltage under different strains and the same illumination power. J_0 is set as the current of the device at zero strain and at reverse applied voltage of 0.5 V. Inset is the configuration of device and direction of forward bias. (d) Characteristic of a piezo-phototronic photodetector based on ZnO nanowires for UV light. The asymmetric change of current under changing strain is clearly demonstrated. Inset is the change of responsivity for forward bias under positive strain.

piezotronics and piezo-phototronics, piezoresistance is always accompanied by the piezoelectric effect.

If piezoresistance effect occurs, the change of resistance is given by

$$\frac{\delta\rho}{\rho} = \pi \frac{\delta l}{l} \quad (16)$$

where ρ is the resistance of the semiconductor, l is the original length of the nanowire, $\delta\rho$ is the resistance change due to piezoresistance effect, δl is the change in nanowire length, and π is the piezoresistance coefficient. From Equation (16) we can see that the piezoresistance is a resistance effect that is uniform and symmetric regardless of the bias of the applied voltage.

2) Effect of series resistance

There are a lot of factors that result in deviation of *I-V* characteristic from ideal current-voltage equation, and one of the most important factors should be the effect of series resistance. Series resistance is the equivalent resistance of various factors in the electric circuit, including outer circuit resistance, capacitors and inductors. Methods to solve the influence of series resist-

ance have been extensively developed.^[24,25] According to these solutions, when applied voltage is small, the device behavior is dominated by current equations for contact junction, including Equation (1) and (2); when applied voltage is large, the device behavior is mostly linear.

Other factors also include the surface trapped charges on the contact areas and the change in contact areas due to externally applied strain. These factors either show a similar behavior to the piezoresistance effect or should be too small to affect the results.

In our model and experiments we successfully demonstrate the difference between the piezo-phototronics effect and other non-piezoelectric effects in highly sensitive photodetection. Here we propose three criteria for characterizing piezo-phototronic photodetection.

- i) Piezo-phototronic photodetection requires the presence of a charge barrier, including a Schottky junction, p-n junction, or some special heterostructure.^[4] Recent studies have also shown that a static internal potential field can also be induced due to piezoelectric effect in special structures such as core-shell nanowires made of materials that have a lattice mismatch.^[4] The piezo charges originate from the dipole nature of piezoelectricity, and they accumulate at the ends of the piezoelectric semiconductor nanowire as fixed charges. With the existence of a charge barrier, the small amount of piezo

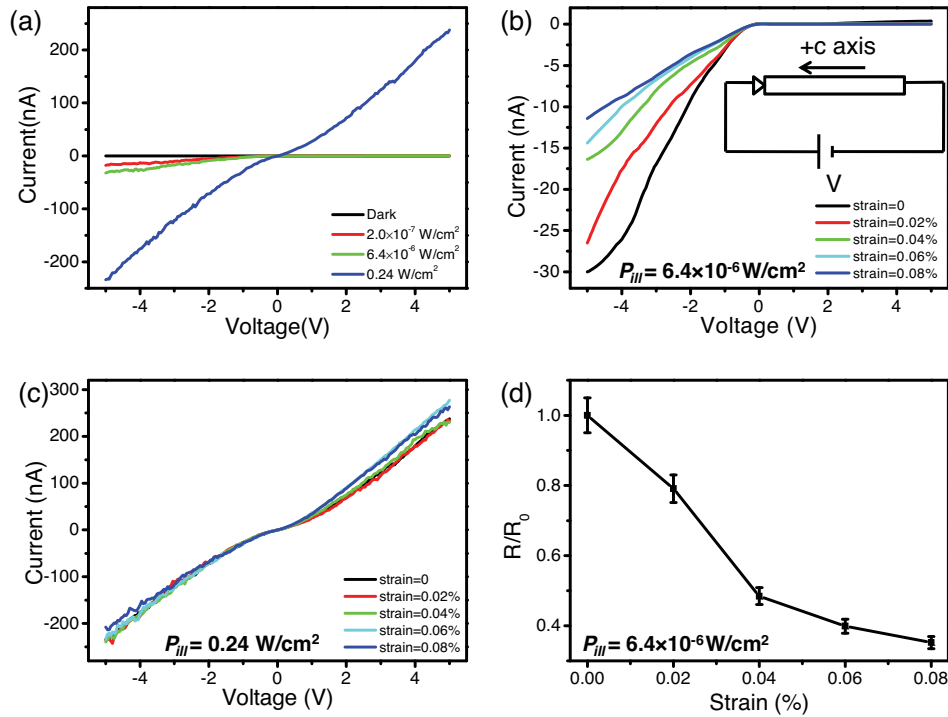


Figure 5. Experimental results for a CdS nanowire MSM photodetector with a single Schottky contact. Light illumination with monochromatic blue light centered at 486 nm. (a) Current-voltage characteristic under different illumination power. Inset it dark current without strain. (b) Current-voltage characteristic under different strain when illumination power is $6.4 \times 10^{-6} \text{ W/cm}^2$. Inset is the configuration of device and direction of forward bias. (c) Current-voltage characteristic under different strains when illumination power is 0.24 W/cm^2 . (d) Calculated relative responsivity under various applied strain when illumination power is $6.4 \times 10^{-6} \text{ W/cm}^2$. R_0 is set as responsivity under zero strain for this illumination power.

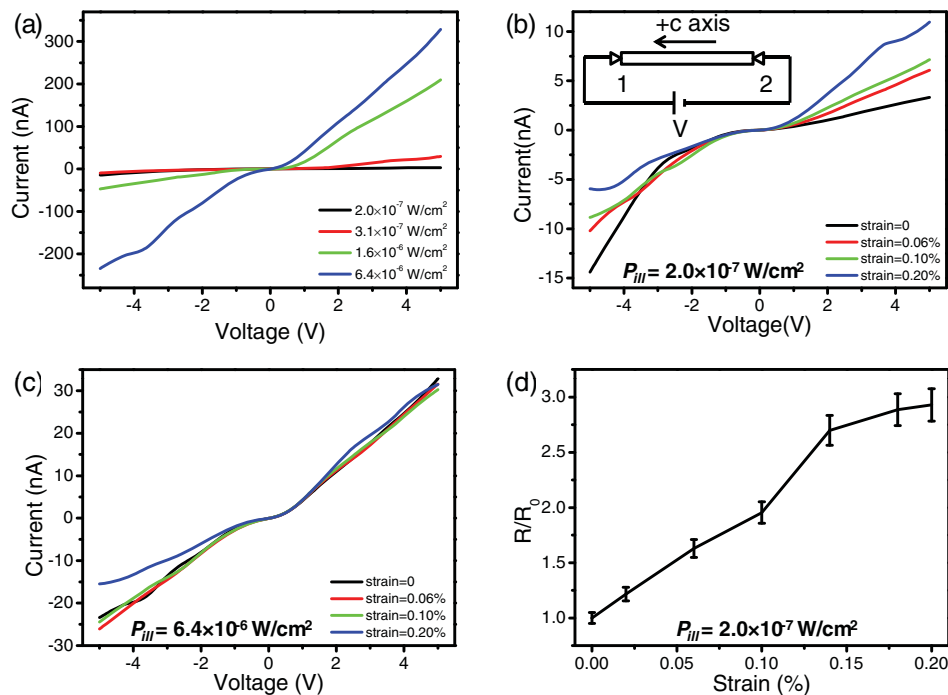


Figure 6. Experimental results for a CdS nanowire MSM photodetector with double Schottky contacts. Light illumination with monochromatic blue light centered at 486 nm. (a) Current-voltage characteristic under different illumination power. (b) Current-voltage characteristic under different strain when illumination power is $2.0 \times 10^{-7} \text{ W/cm}^2$. Inset is the configuration of device and direction of forward bias. (c) Current-voltage characteristic under different strains when illumination power is $6.4 \times 10^{-6} \text{ W/cm}^2$. (d) Calculated relative responsivity under various applied strain when illumination power is $2.0 \times 10^{-7} \text{ W/cm}^2$. R_0 is set as responsivity under zero strain for this illumination power.

charges can effectively tune the current transport properties of the photodetector.

- ii) Photoexcitation influences the current–voltage characteristic through generating excess free charges. Provided that the entire device is under uniform illumination, photon generation of electrons and holes effectively tunes a quasi-Fermi level, and this change is applied along the entire wire, resulting in a decrease of the barrier height.
- iii) Piezoelectric effect influences photodetection by strain induced polar charges at the ends of the nanowires. The effect of piezo-charges in a double Schottky contact photodetector shall result in asymmetric change in barrier heights at the two sides. Other factors induced by external strain such as piezoresistance or contact area change will induce symmetric change in both ends of the nanowire. In this way, we can easily tell whether the change is caused by a genuine piezo-phototronics effect.

These three criteria give a better understanding of our piezo-phototronics experiments, and work as guidance for our future work in related areas. It is also possible to extrapolate our assumption onto other piezo-phototronics phenomena such as piezo-phototronic LED or photocell, and similar conclusion should be retrieved.

Summarizing, we have constructed a theoretical model for piezo-phototronic photodetectors based on metal-piezoelectric semiconductor-metal structures. The model works well with the experiments results on piezopotential enhanced photodetector based on ZnO nanowires in ultraviolet wavelength range and CdS nanowires in visible wavelength range. We have then discussed other factors in the experiments and concluded three criteria based on the physics of piezo-phototronic photodetectors, to differentiate the piezo-phototronic effect from other effects. These criteria support our previous experimental results, and can give guidance to future experiments.

Supporting Information

Supporting Information is available from the Wiley Online Library or from the author.

Acknowledgements

Research was supported by Airforce, U.S. Department of Energy, Office of Basic Energy Sciences, Division of Materials Sciences and Engineering under Award DE-FG02-07ER46394, and NSF (CMMI 0403671). Q.Y. is grateful for the partial support from the National Natural Science Foundation of China (No. 61177062).

Received: November 11, 2011

Revised: December 31, 2011

Published online:

- [1] Y. Hu, Y. L. Chang, P. Fei, R. L. Snyder, Z. L. Wang, *ACS Nano* **2010**, *4*, 1234.
- [2] Z. L. Wang, *Nano Today* **2010**, *5*, 540.
- [3] Y. F. Lin, J. Song, Y. Ding, S. Y. Lu, Z. L. Wang, *Adv. Mater.* **2008**, *20*, 3127.
- [4] F. Boxberg, N. Sondergaard, H. Q. Xu, *Nano Lett.* **2010**, *10*, 1108.
- [5] Z. L. Wang, *Nano Today* **2010**, *5*, 540.
- [6] Q. Yang, X. Guo, W. H. Wang, Y. Zhang, S. Xu, D. H. Lien, Z. L. Wang, *ACS Nano* **2010**, *4*, 6285.
- [7] Y. Hu, Y. Zhang, Y. Chang, R. L. Snyder, Z. L. Wang, *ACS Nano* **2010**, *4*, 4220.
- [8] Q. Yang, W. H. Wang, S. Xu, Z. L. Wang, *Nano Lett.* **2011**, *11*, 4012.
- [9] Y. F. Gao, Z. L. Wang, *Nano Lett.* **2007**, *7*, 2499.
- [10] Y. F. Gao, Z. L. Wang, *Nano Lett.* **2009**, *9*, 1103.
- [11] Z. Gao, J. Zhou, Y. Gu, P. Fei, Y. Hao, G. Bao, Z. L. Wang, *J. Appl. Phys.* **2009**, *105*, 113707.
- [12] Y. Zhang, Y. Liu, Z. L. Wang, *Adv. Mater.* **2011**, *23*, 3004.
- [13] S. M. Sze, *Physics of semiconductor devices*, 2nd ed., Wiley, New York, **1981**.
- [14] E. H. Rhoderick, R. H. Williams, *Metal-Semiconductor Contact*, Clarendon, Oxford **1988**.
- [15] Z. Zhang, K. Yao, Y. Liu, Ch. Jin, X. Liang, Q. Chen, L.-M. Peng, *Adv. Funct. Mater.* **2007**, *17*, 2478.
- [16] D. A. Neamen, *Semiconductor Physics and Devices*, 3rd ed., McGraw-Hill Science/Engineering/Math, **2002**.
- [17] D. G. Thomas, J. J. Hopfield, *Phys. Rev.* **1959**, *116*, 573.
- [18] H. P. Li, C. H. Kam, Y. L. Lam, W. Ji, *Opt. Commun.* **2001**, *190*, 351.
- [19] X. J. Zhang, W. Ji, S. H. Tang, *J. Opt. Soc. Am. B.* **1997**, *14*, 1951.
- [20] Z. W. Pan, Z. R. Dai, Z. L. Wang, *Science* **2001**, *291*, 1947.
- [21] F. X. Gu, Z. Y. Yang, H. K. Yu, J. Y. Xu, P. Wang, L. M. Tong, A. L. Pan, *J. Am. Chem. Soc.* **2011**, *133*, 2037.
- [22] P. W. Bridgman, *Phys. Rev.* **1932**, *42*, 858.
- [23] C. S. Smith, *Phys. Rev.* **1954**, *94*, 42.
- [24] H. Norde, *J. Appl. Phys.* **1979**, *50*, 5052.
- [25] C. D. Lien, F. C. T. So, M. A. Nicolet, *IEEE Trans. Electron Dev.* **1984**, *31*, 1502.